

# Enhanced Topological Graphs for 2-D Sensor Networks

<sup>1</sup>Tarek El Salti,<sup>1</sup>Nidal Nasser, <sup>2</sup>Tarik Taleb, and <sup>3</sup>Anwar Al-Yatama

<sup>1</sup>Department of Computing and Information Science, University of Guelph, Guelph, Ontario, Canada (telsalti; nnasser@uoguelph.ca)

<sup>2</sup>NEC Europe Ltd (tarik.taleb@nw.neclab.eu)

<sup>3</sup>Department of Computer Engineering, Kuwait University (a.yatama@ku.edu.kw)

**Abstract**—For an efficient usage of the sensor technology, several design factors (e.g., topology and sensing coverage) should be taken into account. In this paper, we focus on the underlying topology of sensor networks in two-dimensional environments and enhance a set of recently proposed graphs [1]. The new enhanced graphs are referred to as the Derived Circles version 2 ( $DC^\alpha v2$ ) graphs. We show that  $DC^\alpha v2$  graphs are locally constructed, connected, have the rotation-ability property, and have the Euclidean Minimum Spanning Tree (EMST) as their subgraphs. Moreover, we show that the new set of graphs has a bounded Euclidean/length and power dilation when  $0.5 \leq \alpha \leq 1$ . Furthermore, via simulations, we confirm most of these properties, and demonstrate that the  $DC^\alpha v2$  graphs also have bounded Euclidean and power dilations when  $0 < \alpha < 0.5$ . In addition, we demonstrate that  $DC^\alpha v2$  graphs outperform the Half Space Proximal (HSP) and the Relative Neighbourhood Graph (RNG) graphs in terms of the network dilation, Euclidean dilation, and power dilation. This, in turn, increases the speed for message delivery, reduces the energy consumption of nodes and accordingly prolongs the network lifetime.

## I. INTRODUCTION

There are various topological graphs used in sensor networks. These topologies determine the neighbouring nodes of a given node. Among all the topologies, the Unit Disk Graph (UDG) is a common graph that has been widely used for routing where this functionality is one of the challenging design factors of sensor networks. Unfortunately, routing on UDG is not efficient since it keeps all the edges that can be constructed between a node and its surrounding nodes. Therefore, the UDG maybe considered a dense graph (i.e., its number of edges is close or equal to the maximum number of edges). As a result, running routing protocols based on UDG takes considerable time to choose the next forwarding hop. Moreover, having more edges makes several routing protocols [14], [15] to have a significant delay in their routing procedures (i.e., broadcasts). However, controlling the degree of nodes has recently created the interest of studying other significant factors (i.e., dilations (or stretch factors)) [13], [5], [8] where these factors are effected by the degree of nodes improvements. These dilations measure the power consumption and the packet delivery speed for sensor networks.

Another drawback is that routing on *UDG* does not work all the time, since the UDG topology is typically a non-planar topological graph with crossing edges. These edges may cause

some routing protocols (e.g., face-based protocols [7], [16]) to enter loops. Thus, packet delivery is not guaranteed for these protocols. Hence, one of the primary concerns in the area of sensor networks is to develop algorithms that control the network topologies [11], [12]. Given the fact that sensor nodes are operated by limited battery power, have limited amount of memory, and have topologies that are often not available and may be dynamic, localized algorithms with prior knowledge on neighboring nodes up to a fixed number of distant hops, are ideally preferred. The reason for choosing these algorithms is that they have the following properties that are important for sensor network: 1) reducing the degree of nodes, 2) bounding length/Euclidean and power stretch factors [9] [10], 3) being power efficient [10], and 4) having the rotation-ability property: if a graph ( $G$ ) is rotated by an arbitrary angle to form graph ( $G'$ ), then the resulting sub-topological graph of  $G'$  ( $P(G')$ ) is not necessarily a rotation of the sub-topological graph of  $G$  ( $P(G)$ ). Therefore, running a routing protocol on  $P(G)$  may yield different results compared to the same routing protocol running on  $P(G')$ . This actually affects the accuracy of the routing protocol evaluation and thus misjudges the routing protocol performance.

There are various localized topological graph algorithms ([8], [2]). Generally, implementing and running routing protocols on these topologies improve their performance. We are mainly interested in the recently proposed graph, which is referred to as the Half Space Proximal (HSP) graph [8]. The reason for choosing this graph, is that it is considered to be a new graph compared to some other proposed graphs [10] [2]. Moreover, we are interested in the Relative Neighborhood Graph (RNG) [2] since this graph as well as our new set of graphs share the property of having bounded forbidden areas. However, unlike the RNG, the new proposed graphs have dynamic forbidden areas which give all the possibilities for nodes elimination between a current node and its nearest neighboring nodes. The HSP, RNG, and some other existing graphs [10] are proposed for ad hoc networks in general, which can also apply to sensor networks.

An interesting work done by Chavez *et al.* [8] proposes a topological graph referred to as the *Half Space Proximal Graph*  $HSP(G)$ , where  $G$  is a geometric graph. First a directed  $D-HSP(G)$  is defined as follows. At each node  $u$  in  $G$ , the following iterative procedure is performed until all neighbors

of  $u$  are either discarded or are connected with an edge. A directed edge  $(u, v)$  is formed with the nearest neighbor  $v$ . An open half plane is defined by a line perpendicular to  $(u, v)$ , intersecting  $(u, v)$  at its middle point, and containing  $v$ . All nodes in this half plane are then discarded. The procedure then continues with the next nearest non-discarded neighbor and so on until all nodes have been discarded. The selected directed edges determine the  $D\tilde{H}SP(G)$ . The undirected  $HSP(G)$  is obtained by ignoring the direction of the edges, yielding a subgraph that may still have crossing edges. Among the properties shown in [8] for the  $HSP$  subgraph are the following: it is strongly connected, has an out-degree of at most six, contains the Euclidean Minimum Spanning Tree ( $EMST$ ) as its subgraph, and has the rotation-ability property. The main drawback of the  $HSP$  is that it does not have an upper bound for its length stretch factor [5]. Moreover, it does not have an upper bound for its power stretch factor.

Another work done by Toussaint [2] proposes the Relative Neighborhood Graph ( $RNG$ ) that uses a forbidden area to define the edges constructed between a set of nodes, where the edges are considered undirected. The  $RNG$  graph is constructed as follows. An edge binding two vertices,  $u$  and  $v \in V$ , is in  $RNG$  if the intersection of the two circles centred on two vertices each with radius  $|uv|$  does not have any other vertex  $w \in V$ . The  $RNG$  has several properties, and they are as follows. This graph is connected and contains the  $EMST$  as its subgraph [2]. Moreover, this graph has the rotation-ability property. The main drawback of this graph is that it does not have a bounded length and power stretch factor [6] [10]. In this paper, we propose a new set of topological graphs which are referred to as the Derived Circle version 2 ( $DC^\alpha v2$ ) topological graphs, where  $0 \leq \alpha \leq 1$ . These graphs are extended and enhanced from the Derived Circle ( $DC^\alpha$ ) graphs proposed by El Salti *et al.* in [1]. The new graphs permit the control over the degree of the nodes while having the rotation-ability property. Acquiring the rotation-ability preserves the accuracy of the routing protocol regardless of the rotation of the nodes. Furthermore, reducing the degree of nodes increases the speed of the routing decisions performed on the  $DC^\alpha v2$  graph. However, the  $DC^\alpha v2$  graph does not remove too many edges, since there is a need for these edges to improve the different kind of dilations (e.g., Euclidean dilation).

Moreover, the  $DC^\alpha v2$  graphs are shown to be locally constructed, connected, and have the Euclidean Minimum Spanning Tree ( $EMST$ ) as their subgraphs. In addition, we show that the new set of graphs has a bounded Euclidean/length and power dilation when  $0.5 \leq \alpha \leq 1$ . Furthermore, via simulations, we confirm most of these properties, and demonstrate that the  $DC^\alpha v2$  graphs also have bounded Euclidean and power dilations when  $0 < \alpha < 0.5$ . In addition, we demonstrate that  $DC^\alpha v2$  graphs outperform  $HSP$  and  $RNG$  graphs in terms of the network dilation, Euclidean dilation, and power dilation where this is the first time in the literature that the  $HSP$  is evaluated in terms of power dilation. Outperforming the existing topologies in terms of length/Euclidean and power dilations implies that less energy is consumed when forward-

ing a message in the  $DC^\alpha v2$ 's paths, which makes the  $DC^\alpha v2$  to be power-efficient graph. As a consequence, the lifetime of a sensor network is increased. In addition, outperforming the existing topologies in terms of hop and Euclidean dilations implies faster message delivery. All these properties strictly impact the performance of any routing protocol that runs on the  $DC^\alpha v2$  topologies. Therefore, the  $DC^\alpha v2$  graphs are considered power- and time-efficient graphs.

The rest of the paper is organized as follows. Some geometric concepts and metrics used in our proposed graphs are presented in Section II. The Derived Circle ( $DC^\alpha v2$ ) graphs are proposed along their theoretical properties in Section III. The  $DC^\alpha$ 's properties are demonstrated experimentally in Section IV. Finally, concluding remarks are drawn in Section V.

## II. PRELIMNARIES

Before presenting our new set of graphs, we first demonstrate some of the geometric concepts and metrics that are needed as a part of our solution.

### A. Geometric Concepts and Metrics

In our communication model, a graph on the point set  $S$  in 2-D, can be modeled as a weighted (undirected or directed) graph  $G(S, E)$  where  $E$  is the set of edges  $(u, v)$  between nodes  $u$  and  $v \in S$ . The 2-D position of the nodes are assumed to be fixed and known via some positioning techniques proposed in [4]. The weight of an edge  $(u, v)$  is the 2-D Euclidean distance  $|uv|$ . The weight of a graph is the sum of its edge weights. Moreover, in our model, two nodes  $u$  and  $v$ , where  $u \neq v$ , are connected by an undirected edge if the Euclidean distance between them is at most their transmission range ( $R_c$ ). The resulting graph is called a Unit Disk Graph ( $UDG$ ). For each node  $u$ , we denote the set of its neighbors by  $N(u)$ . The number of the neighbors of  $u$  is the degree of  $u$ .

A subgraph of  $G$ ,  $P(G)$ , is defined as  $t$ -spanner of  $G$  if the length of the shortest path between any two nodes in  $P(G)$  is at most  $t$  times the shortest path between them in  $G$ , where  $t$  is the stretch factor or the dilation ratio. The length of a path is divided into three main types: 1) Euclidean path length<sup>1</sup>, 2) network path length, and 3) power path length [10]. The first type refers to the sum of all the hops' Euclidean distances in a path. The second type refers to the hop count of a path. The last type refers to the sum of the consumed energy for the edges in a path referred by  $p(\pi) = \sum_{i=1}^q \|v_{i-1}v_i\|^\beta$ , where  $\pi$  refers to the path,  $q$  refers to the total number of nodes,  $v_i$  refers to a sensor node, and  $\beta$  is a constant parameter from within the interval [2, 4] [10].

## III. DESCRIPTION AND ANALYSIS OF DERIVED CIRCLE VERSION 2 ( $DC^\alpha v2$ ) GRAPHS

Although it was mentioned in [1] that the Derived Circle graphs ( $DC^\alpha$ ) achieve connectivity, we show a counter-example where they fail to achieve such property (see Figure

<sup>1</sup>Usually in the literature, a stretch factor implicitly means Euclidean/length stretch factor. Otherwise the type of stretch factor is specified.

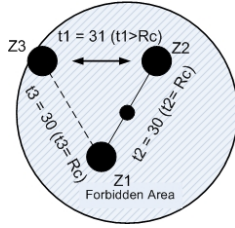


Fig. 1. A counter-example for Theorem 2 in [1].

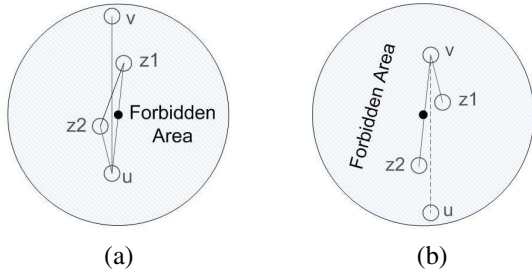


Fig. 2. (a)  $DC^\alpha v_2$  graph chooses the second shortest edge, where  $\alpha = 0.5$ .  
(b) Node  $v$  runs the  $DC^\alpha v_2$  graph with  $\alpha = 0.5$ .

1). In this figure, node  $z_1$  is the current node which arbitrarily chooses the edge with node  $z_2$  as its shortest edge ( $t_2 = t_3$ ). The forbidden area that are displaced along the shortest edge  $t_2$  eliminates the edge  $(z_1, z_3)$ . Additionally, since the distance between  $z_2$  and  $z_3$  is more than the communication range ( $R_c$ ), a disconnected topology is obtained. In this section, we therefore propose a set of enhanced  $DC^\alpha$  referred to as  $DC^\alpha$  version 2 ( $DC^\alpha v_2$ ) which not only achieves connectivity, but also has a bounded Euclidean stretch factor, power stretch factor, and has the Euclidean Minimum Spanning Tree (EMST) as its subgraph.

Each node  $u$  running the  $DC^\alpha v_2$  algorithm chooses a neighbor,  $v$ , from the list of its neighbours  $N(u)$ , that is the nearest neighbouring node to  $u$ . Afterwards, a restricted forbidden area (i.e., circle) is drawn with  $u$  as a center and a radius  $d$ , where  $d$  is the distance between  $u$  and  $v$ . We use the term  $\alpha$  to parameterize the closed line segment between  $u$  and  $v$ :  $(1-\alpha)u + \alpha v$ , where  $0 \leq \alpha \leq 1$ . Any particular choice of  $\alpha$  represents the position of the circle position between  $u$  and  $v$ .

The circle eliminates any edge with a neighbor  $q$  with a specific value of  $\alpha$ , where  $q \neq v$ , that falls into the circle if and only if node  $u$  falls into the forbidden area, displaced with the same value of  $\alpha$ , drawn between  $q$  and its neighbor  $q_1$ , where  $q_1 \neq u$ . We repeat the same process for each sensor node. This is illustrated in Figure 2. Notice that in Figure 2a, the centre of the circle is located at the midway distance between  $u$  and  $z_1$ . Also notice that the circle in Figure 2b is centered at the midway distance between  $v$  and  $z_2$ . The edge between the current node and its nearest neighbor is preserved while eliminating other edges that are longer and satisfy the  $DC^\alpha v_2$ 's criteria. This explains why the edges  $[v, z_1]$ ,  $[v, z_2]$ ,  $[z_1, u]$ , and  $[z_2, u]$  are preserved.

The definition of the  $D-DC^\alpha v_2$  (the directed version) is

summarized as follows.

*Definition 1:* Let  $G$  be a UDG with node set  $S$ . The directed  $D-DC^\alpha v_2$  subgraph is defined as the graph with node set  $S$  whose edges are obtained by applying the  $DC^\alpha v_2(G)$  algorithm on graph  $G$  using displacement parameter  $\alpha$ .

Referring to the above definition, the undirected graph  $DC^\alpha v_2(G)$  is obtained by ignoring the direction of the edges in  $D-DC^\alpha v_2$ . In this paper, we are interested in the undirected version. However, when setting  $\alpha = 0$ , we simply refer to the resultant graph as the  $UDG$  graph. This can be explained as follows. When  $\alpha$  is equal to zero,  $DC^\alpha v_2(G)$  does not eliminate edges, since there will be no neighbouring node  $z$ , closer to node  $u$  than node  $v$ . The same applies when  $\alpha$  is very small, however, the  $DC^\alpha v_2(G)$  may or may not eliminate edges. Notice that the directions of the nearest neighbor do not effect the construction of the  $DC^\alpha v_2$  graphs. Therefore, the resultant subgraph is the same regardless of the orientation of the point set  $S$ . Hence, the  $DC^\alpha v_2(G)$  has the rotation-ability property. The running time of the algorithm per node is  $O(l^2)$  where  $l$  is the degree of the node. After giving detailed description of the  $DC^\alpha v_2$  graphs, along with the rotation-ability property, we show additional properties for the  $DC^\alpha v_2$  graphs as follows. The new proposed theorems replace all the theorems proposed in [1] since one of the new theorems reprove the connectivity property, while the other theorems are more important than those previously proposed in terms of topology's properties.

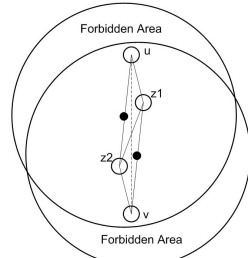


Fig. 3. A proof for Theorem 1.

*Theorem 1:* If  $G$  is a connected UDG, then the  $DC^\alpha v_2$  graph is also connected when  $0 < \alpha \leq 1$ .

*Proof:* Assume that for every edge between a pair of nodes in UDG,  $\nexists$  any path  $\vec{P}$  between these end nodes in the  $DC^\alpha v_2$  graph. Taking one edge, say  $[u, v]$  in UDG,  $\nexists$  any path  $\vec{P}$  between these nodes in the  $DC^\alpha v_2$  graph (see Figure 3). One possibility for this is that  $\exists$  a node  $z_1:|z_1u| = H_1|z_1v|$ , where  $0 < H_1 \leq 0.5$ ,  $|z_1v| \leq R_c$ , and  $|z_1v| \leq |uv|$ , respectively. In addition,  $\exists$  another node  $z_2:|z_2v| = H_2|z_2u|$ , where  $0 < H_2 \leq 0.5$ ,  $|z_2u| \leq R_c$ ,  $|z_2u| \leq |uv|$ , respectively. Thus, all these distances represent edges in  $G$  (UDG), and remain in the  $DC^\alpha v_2$  graph. However, the edge  $[u, v]$  is eliminated when  $H_1 = H_2 = 0.5$  for  $0.5 \leq \alpha \leq 1$ , and the more  $H_1$  and  $H_2$  decreases ( $< 0.5$ ), the more the values for  $\alpha$  ( $< 0.5$ ) would enable the  $DC^\alpha v_2$  to eliminate the edge

<sup>2</sup>H1 and H2 are assumed to be equal.

$[u,v]$ . Therefore, even though the edge  $[u,v]$  can be eliminated  $\forall \alpha, \exists \vec{P}$  between  $u$  and  $v$  in  $DC^\alpha v2$ . This represents a contradiction. ■

*Theorem 2:* If  $G$  is a connected UDG, then a Euclidean Minimum Spanning Tree ( $T$ ) of  $G$  is a subgraph of the  $DC^\alpha v2$  graph, where  $0 < \alpha \leq 1$ .

*Proof:* This proof is based on the proof presented in [8], and it is as follows. Assume that  $\exists$  edge  $[u,v]$  in  $T$ , but  $\notin$  in the  $DC^\alpha v2$  graph. In addition,  $T$  does not include the edges  $[u, z1]$ ,  $[u, z2]$ ,  $[v, z1]$ , and  $[v, z2]$ . The possibility for not having the edge  $[u,v]$  in the  $DC^\alpha v2$  graph is similar to the possibility mentioned in the previous proof using nodes  $z1$  and  $z2$ . Based on the fact that the  $T$  is connected, there should be a path  $\vec{P}$  from  $u$  to  $z1$  in  $T$  (via some nodes not shown in Figure 3). Thus, removing the edge  $[u,v]$  from  $T$  and adding the edge  $[z1,v]$  from the  $DC^\alpha v2$  graph to  $T$  results in a new  $T'$  which has lower or equal weight ( $W^+$ ) to  $T$ , a contradiction. Also, there should be a path  $\vec{P}$  from  $v$  to  $z1$  in  $T$  (via some nodes not shown in Figure 3). Thus, removing the edge  $[u,v]$  from  $T$  and adding the edge  $[z1,u]$  from the  $DC^\alpha v2$  graph to  $T$  results in a new  $T'$  which has lower or equal  $W^+$  to  $T$ . This represents a contradiction. The same applies to paths from  $u$  to  $z2$ , and from  $v$  to  $z2$ . ■

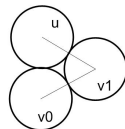


Fig. 4. A proof for Theorem 3.

*Theorem 3:* Let  $G$  be a geometric 2-D UDG and the  $DC^\alpha v2$  graph is a subgraph of UDG. Then, the stretch factor of the  $DC^\alpha v2$  graph, when  $0.5 \leq \alpha \leq 1$ , is at most two.

*Proof:* Assume the following. Node  $u = v(k+1)$  is connected to node  $v0$  in UDG, and nodes  $v1, v2, \dots, vk$  are between  $v0$  and  $v(k+1)$ . For simplicity, we assume  $k = 2$ , and  $R_c = 1$ . The term  $R_c$  is calculated based on the sensing range ( $R_c = 2 * R_s$  [3]). In addition, the edge  $[u, v0] \in$  UDG but  $\notin DC^\alpha v2$  graph. We mention the worst case and it is as follows (see Figure 4).  $\exists$  node  $v1$  that has an edge with  $u ([u, v1])$  of length equal to the length of the edge between  $v1$  and  $v0$  ( $[v0, v1]$ ), and the length of these edges is equal to  $R_c$ . Thus,  $\notin$  edge  $[u, v0] \in DC^\alpha v2$  graph since placing a circle (forbidden area) between  $u$  (current node) and  $v1$  (its neighbor), where  $0.5 \leq \alpha \leq 1$ , eliminates node  $v0$  from node  $u$ 's list of neighbor. In order to complete the condition for  $[u, v0]$  elimination, a circle is placed between  $v0$  (current node) and  $v1$  (its neighbor) with  $\alpha$  equal to the  $\alpha$  between  $u$  and  $v1$ . This eliminates  $u$  from node  $v0$ 's list of neighbors. The Euclidean length (sum of Euclidean distances) between  $u$  and  $v0$  in the  $DC^\alpha v2$  graph is therefore bounded by a constant. Thus, the maximum stretch factor for the  $DC^\alpha v2$  graph when  $0.5 \leq \alpha \leq 1$  is always less than  $2R_c = 2(1) = 2$ . ■

*Theorem 4:* Let  $G$  be a geometric 2-D UDG and the  $DC^\alpha v2$  graph is a subgraph of UDG. Then, the power stretch

factor of the  $DC^\alpha v2$  graph, when  $0.5 \leq \alpha \leq 1$ , is at most  $2^\beta$ , where  $\beta$  is a constant parameter from within the interval  $[2, 5]$ .

*Proof:* Based on Lemma 2 in [10], a topological graph with a stretch factor of at most  $y$  has a power stretch factor of at most  $y^\beta$ . ■

#### IV. PERFORMANCE EVALUATION

In this section, we evaluate the performance of the  $DC^\alpha v2$  graphs and compare them to  $HSP$  and  $RNG$  graphs [8] [2]. We first present the simulation model used along with the evaluation metrics. Later, we show and discuss the obtained simulation results.

##### A. Simulation Model

In our experiments, we used randomly connected Unit Disk Graphs ( $UDG$ ) on an area of  $100 \text{ m} \times 100 \text{ m}$ . We varied the number of nodes,  $n$ , between 65, 75, 85, 95, and 105 nodes. For each  $UDG$ ,  $DC^\alpha v2$  graphs with  $\alpha = 0.25$ ,  $\alpha = 0.50$ ,  $\alpha = 0.75$ ,  $\alpha = 1.0$ ,  $HSP$ , and  $RNG$  are all generated. The  $DC^\alpha v2$ , where  $\alpha=0$ , is not evaluated since the graph is obviously the same as the UDG graph. We set the transmission range  $R_c$  to 15 units in all tested graphs. Furthermore, all the obtained results are averaged over 22 graphs<sup>3</sup>.

##### B. Performance Evaluation Metrics

There are two main metrics used in our experiments. The first metric is called the dilation and it is defined as follows.  $P(G)$  refers to a subgraph of  $G$ , where  $G$  is the  $UDG$ .  $P(G)$  is considered to be a  $t$ -spanner of  $G$  if the length of the shortest path between any two nodes in  $P(G)$  is at most  $t$  times the shortest path between them in  $G$ , where  $t$  is the stretch factor or the dilation ratio. There are three types of dilations: 1) the hop/network dilation, 2) the Euclidean/length dilation, and 3) the power dilation. In this paper, we set the parameter  $\beta$  that is used in the power dilation to two. However, we study the upper and average bounds for the network, Euclidean, and power dilations in order to find out the worst and general behaviors for the  $DC^\alpha v2$  graphs. The second metric is the average node degree, where the node degree refers to the number of neighbors of a particular node.

##### C. Simulation Results

From Figure 5, it is shown that even though the  $DC^\alpha v2$  graphs, where  $0 \leq \alpha \leq 1$ , do not outperform  $HSP$  and  $RNG$  in terms of the average node degree, they outperform  $UDG$ . In particular, the  $DC^\alpha v2$  graphs perform much better when  $\alpha > 0$ . This is because as  $\alpha$  increases, the circle drawn in  $DC^\alpha v2$  has more chances to eliminate more edges. However, as  $\alpha$  reaches the value of one,  $DC^\alpha v2$  can still remove edges, but at the same time, there is a possibility that the circle does not contain anymore neighboring nodes that used to be in the circle when  $\alpha$  is smaller. This explains why the  $DC^\alpha v2$  graphs, when  $\alpha = 0.5, 0.75, 1$ , exhibit similar performance in terms of the average node degree.

<sup>3</sup>Confidence level is 95%.

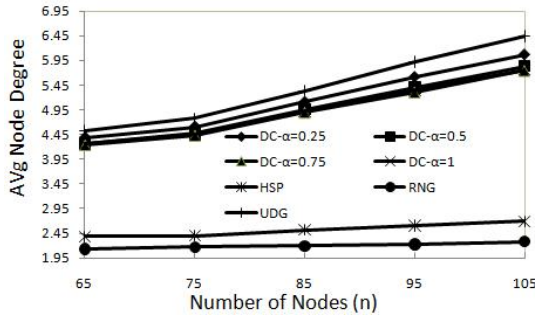


Fig. 5. Average node degree.

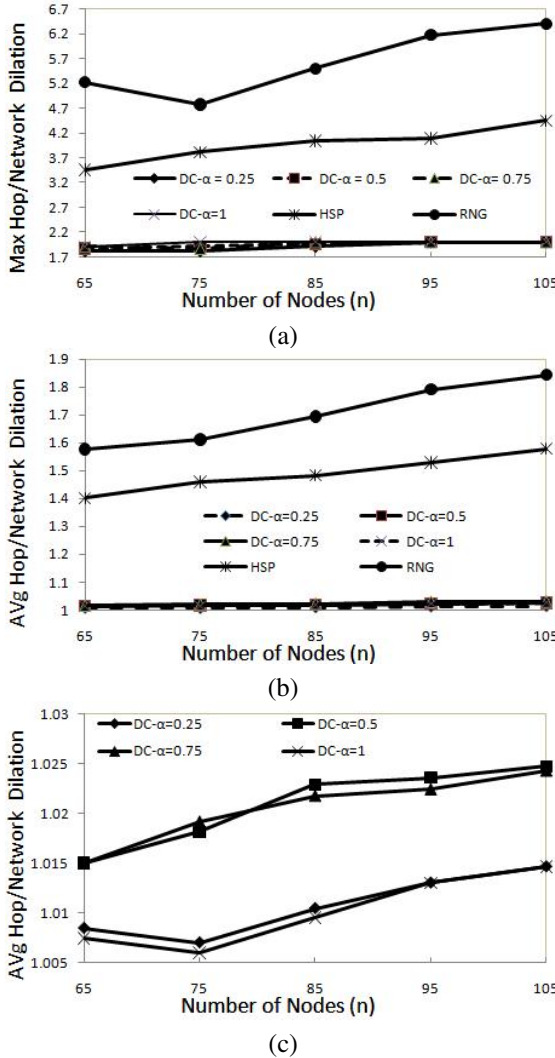
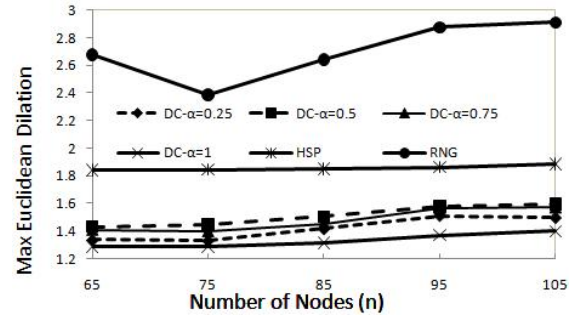
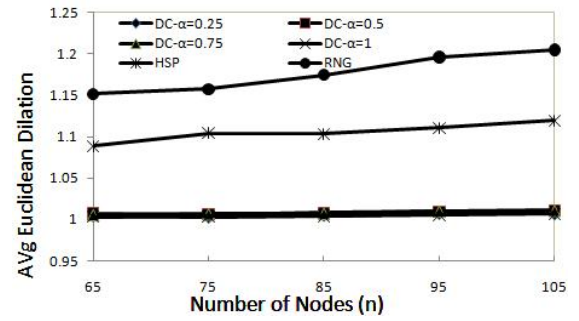


Fig. 6. (a) Maximum network dilation. (b) Average network dilation. (c) Average network dilation for only  $DC^\alpha v2$  graphs.

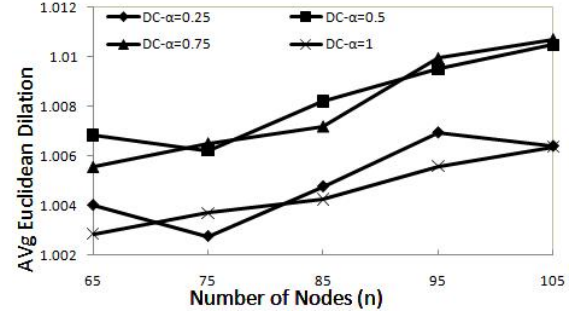
From Figures 6 and 7, the  $DC^\alpha v2$  graphs outperform the *HSP* and *RNG* graphs in terms of network and Euclidean dilations (both maximum and average dilations). This can be seen for all simulated values of  $\alpha$ . We explain this behavior based on Figure 5 as follows. As  $\alpha$  increases, the  $DC^\alpha v2$  graphs eliminate more edges. But since these graphs deal with



(a)



(b)



(c)

Fig. 7. (a) Maximum Euclidean dilation. (b) Average Euclidean dilation. (c) Average Euclidean dilation for only  $DC^\alpha v2$  graphs.

a forbidden restricted area (i.e., circle), they do not eliminate too many edges as *HSP* and *RNG* do. Therefore, more edges exist in the  $DC^\alpha v2$  graphs. This implies that the  $DC^\alpha v2$  graphs have higher possibility to find shorter paths than in the case of the *HSP* and *RNG* graphs.

Additionally, there is another interesting behavior for the  $DC^\alpha v2$  graphs, which is clearly shown in Figure 6c, Figure 7c, respectively. As  $\alpha$  increases, the dilation increases, however, when  $\alpha$  reaches the value of one, there is a reflection in the  $DC^\alpha v2$ 's behavior; i.e., the dilation decreases. The reason for this behavior is that as  $\alpha > 0.5$ , the circle drawn starts to loose some nodes that were in the interior of the circle, and more edges are consequently constructed. Hence, there is a higher possibility to find shorter paths. This makes  $DC^\alpha v2$  with  $\alpha = 1$  retrieve most of the short paths removed by  $DC^\alpha v2$  with  $\alpha = 0.25$ , which explains the low values for both network and Euclidean dilations for  $DC^\alpha v2$  with  $\alpha = 1$ .

As it can be seen from Figure 8 (both maximum and

average dilations), the  $DC^{\alpha}v2$  graphs outperform *HSP* and *RNG* in terms of the power dilation. This is due to the fact that the  $DC^{\alpha}v2$  graphs, where  $0 \leq \alpha \leq 1$ , have smaller Euclidean dilations than *HSP* and *RNG* (see Figure 7). This means that the  $DC^{\alpha}v2$  graphs, where  $0 \leq \alpha \leq 1$ , consume less energy (i.e., battery power) of the sensor nodes than the *HSP* and *RNG* graph do. This good performance contributes to prolonging the lifetime of the network which makes the  $DC^{\alpha}v2$  graphs to be power-efficient.

It is also worth mentioning that the maximum Euclidean and power dilations for the  $DC^{\alpha}v2$  graphs when  $0.5 \leq \alpha \leq 1$  is below a constant, which adequately validates Theorem 3 and Theorem 4, respectively. Moreover, the experiments demonstrate that the  $DC^{\alpha}v2$  graphs, when  $0 < \alpha < 0.5$ , has maximum Euclidean and power dilations that are below a constant. Another point to mention is that from our experiments, we found that all the tested  $DC^{\alpha}v2$  graphs, where  $0 \leq \alpha \leq 1$ , always remain connected. Thus, Theorem 1 is also confirmed.

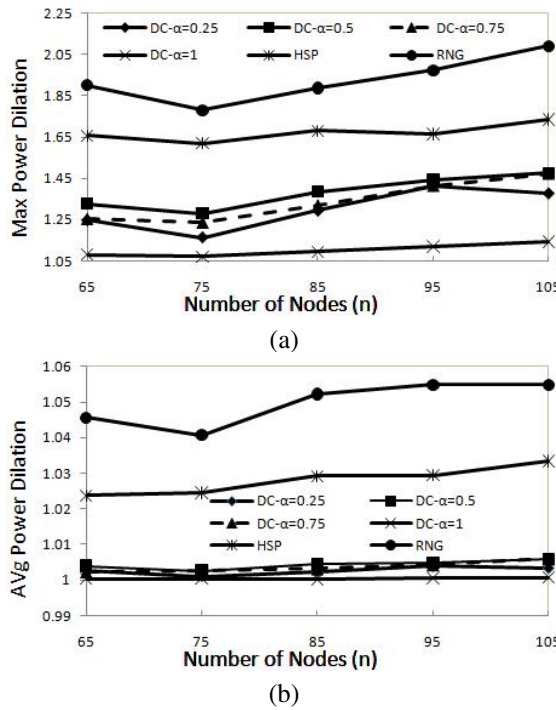


Fig. 8. (a) Maximum power dilation. (b) Average power dilation.

## V. CONCLUSIONS

In this paper, we proposed a set of topological graphs which are referred to as the Derived Circle ( $DC^{\alpha}v2$ ). We have shown that the  $DC^{\alpha}v2$  graphs are locally constructed, connected, power-efficient, have a bounded Euclidean and power dilations, and have the rotation-ability property. Furthermore, we demonstrated via computer simulations that the  $DC^{\alpha}v2$  graphs outperform *HSP* and *RNG* in terms of the network, Euclidean, and power dilations. Achieving low network dilations improves the performance of the underlying routing protocol in terms of data transmission latency.

Furthermore, achieving low Euclidean dilation also shortens the time for message delivery. This is in accordance with the previous results obtained when measuring the network dilation. In addition, achieving low Euclidean dilation strictly means that the energy spent for transmitting a message from one sensor node to another is low. This reduces the energy consumption of the overall sensor networks, which therefore, prolongs the lifetime of the network. Lastly, it is obvious that when achieving low power dilation, the energy consumption would be low. For future work, we will study routing based on these new topologies.

## REFERENCES

- [1] T. El Salti, N. Nasser, and T. Taleb. A Set of Topological Graphs for 2-D Sensor Ad Hoc Networks. *IEEE International Conference on Communications (ICC)*, Dresden, Germany, June 2009.
- [2] Toussaint, G. The relative neighborhood graph of finite planar set. *Pattern Recognition*, vol. 12, no. 4, pages 261–268, 1980.
- [3] Xing, G. and Lu, C. and Pless, R. and Huang, Q. Impact of sensing coverage on greedy geographic routing algorithms. *IEEE Transactions on Parallel and Distributed Systems*, vol. 17, no. 4, pages 348–360, April 2006.
- [4] V. Chandrasekhar, W. KG Seah, Y. Sang Choo, and H. Voon Ee. Localization in underwater sensor networks: survey and challenges. In *Proceedings of the 1st ACM international workshop on Underwater networks*, pages 33–40, Los Angeles, CA, USA, Sept. 2006.
- [5] P. Bose, P. Carmi, M. Couture, M. Smid, and D. Xu. On a family of strong geometric spanners that admit local routing strategies. In *Proceedings of the Workshop of Algorithms and Data Structures (WADS)*, pages 300–311, Portland, Oregon, USA, 2007.
- [6] P. Bose, L. Devroye, W. Evans, and D. Kirkpatrick. On the Spanning Ratio of Gabriel Graphs and beta-Skeletons. *SIAM J. Discret. Math.*, vol. 20, no. 2, pages 412–427, Philadelphia, PA, USA, 2006.
- [7] P. Bose, P. Morin, I. Stojmenović, and J. Urrutia Routing with guaranteed delivery in ad hoc wireless networks. *Wirel. Netw.*, Kluwer Academic Publishers, Hingham, MA, USA, vol. 7, no. 6, 2001, pp. 609–616.
- [8] E. Chavez, S. Dobrev, E. Kranakis, J. Opatrný, L. Stacho, H. Tejeda, and J. Urrutia. Half-space proximal: A new local test for extracting a bounded dilation spanner. In *Proc. of the International Conference On Principles of Distributed Systems (OPODIS 2005)*, vol. 3974 of LNCS, pages 235–245, Pisa, Italy, 2006.
- [9] X.-Y. Li, G. Călinescu, and P.-J. Wan. Distributed construction of a planar spanner and routing for ad hoc wireless networks. In *Proc. of INFOCOM'2002*, vol. 3, pages 1268–1277, 2002.
- [10] X.-Y. Li, P.-J. Wan, and Y. Wang. Power efficient and sparse spanner for wireless ad hoc networks. In *Proc. of IEEE Int. Conf. on Computer Communications and Networks (ICCCN01)*, pages 564–567, Scottsdale, AZ, USA, 2002.
- [11] X.Y. Li. *Topology Control in Wireless Ad Hoc Networks*. IEEE Press, 2003.
- [12] R. Rajaraman. Topology control and routing in ad hoc networks: A survey. *ACM SIGACT News*, vol. 33, no. 2, pages 60–73, June 2002.
- [13] Dumitrescu, Adrian and Tóth, Csaba D. Light orthogonal networks with constant geometric dilation. *J. of Discrete Algorithms*, vol. 7, no. 1, pages 112–129. Elsevier Science Publishers B. V., Amsterdam, The Netherlands, 2009.
- [14] Saad, C.; Benslimane, A.; Champ, J.; Konig, J.-C. Ellipse Routing: A Geographic Routing Protocol for Mobile Sensor Networks with Uncertain Positions. *IEEE Global Telecommunications Conference (GLOBECOM)*, pages 1–5, New Orleans, LA, USA, 2008.
- [15] Ko, Y. and Vaidya, N. H. Location-aided routing (LAR) in mobile ad hoc networks. *Wirel. Netw.*, vol. 6, no. 4, pages 307–321, Kluwer Academic Publishers, Hingham, MA, USA, 2000.
- [16] Karim Seada, Ahmed Helmy. Efficient and robust geocasting protocols for sensor networks. *Computer Communications*, vol. 29, no. 2, pages 151–161, Elsevier Science Publishers B. V., The Netherlands, Jan. 2006.